

Chargino reconstruction in supersymmetry with long-lived staus

Sanjoy Biswas* and Biswarup Mukhopadhyaya†

Regional Centre for Accelerator-based Particle Physics, Harish-Chandra Research Institute, Chhatnag Road, Jhansi, Allahabad - 211 019, India

(Received 3 November 2009; published 7 January 2010)

We consider a supersymmetric (SUSY) scenario including right-handed neutrinos, one of whose scalar superpartners is the lightest SUSY particle. The distinguishing feature in the collider signal of SUSY in such a case is not missing energy but a pair of charged tracks corresponding to the next-to-lightest SUSY particle, when it is, as in the case considered, a stau. Following up on our recent work on neutralino reconstruction in such cases, we explore the possibility of reconstructing charginos, too, through a study of transverse mass distributions in specified final states. The various steps of isolating the transverse momenta of neutrinos relevant for this are outlined, and regions of the parameter space where our procedure works are identified.

DOI: 10.1103/PhysRevD.81.015003

PACS numbers: 12.60.Jv

I. INTRODUCTION

If supersymmetry (SUSY) [1,2], broken at the TeV scale, has to validate itself as the next step in physics beyond the standard model (SM), then it is likely to be discovered at the Large Hadron Collider (LHC), with the superpartners of the SM particles being identified. It is therefore of great importance to make a thorough inventory of collider signals answering to various SUSY scenarios. These can serve not only to unveil the general character of the scenario but also to yield a wealth of information about the specific properties of the new particles.

One attractive feature of supersymmetric theories, in the R -parity [defined as $R = (-)^{3B+L+2S}$] conserving form, is that the superparticles are always produced in pairs and each interaction vertex must involve an even number of superparticles (having $R = -1$). Hence the lightest SUSY particle (LSP) is stable and all SUSY cascades at the collider experiments should end up with the pair production of the LSP. As a bonus, it provides a viable candidate for dark matter if the LSP is electrically neutral and only weakly interacting. Since the LSP, due to such a character, escapes the detector without being detected, a prototype signature of R -conserving SUSY is energetic jets and/or leptons associated with large missing transverse energy (\cancel{E}_T).

However, there can be several SUSY models [3] which include a quasistable next-to-lightest supersymmetric particle (NLSP). This can happen in cases where the NLSP is nearly degenerate in mass with the LSP, or if its coupling to the LSP is too small. Hence the decay width of the NLSP into the LSP is highly suppressed. Consequently the NLSP becomes stable on the detector scale, its lifetime being long enough to escape the detector without decaying inside it. Thus the NLSP behaves like a stable particle within the

detector. The resulting collider signals change drastically, especially if the NLSP is a charged particle. The quintessential SUSY signal then is not \cancel{E}_T but two hard charged tracks of massive stable particles which appear as far as up to the muon chamber. This opens up a whole set of new possibilities for collider studies, including reconstruction of the sparticle masses, something that is relatively more difficult in the presence of \cancel{E}_T .

The scenario we have considered here, as an illustration of such a quasistable NLSP, is the minimal supersymmetric standard model (MSSM) augmented with a right-chiral Dirac-type neutrino superfield for each generation. This is consistent with the existing evidence [4] of neutrino masses and mixing, although no explanation for the smallness of neutrino masses is offered. It is possible in such a case to have a LSP that is dominated by this right-chiral sneutrino state ($\tilde{\nu}_R$) together with a charged particle as the NLSP. We specifically consider a situation with a stau ($\tilde{\tau}$) NLSP.¹ Such a scenario can easily be motivated [7] by assuming that the MSSM is embedded in a high-scale framework of SUSY breaking. As we shall see, this can happen in minimal supergravity (mSUGRA) [8] where the masses evolve from “universal” scalar (m_0) and gaugino ($M_{1/2}$) mass parameters at a high scale. The only extension here is the right-chiral neutrino superfield (in fact, three of them) whose scalar component derives its soft mass from the same m_0 . The existence of such a quasistable charged slepton can be well in agreement with the observed abundance of light elements as predicted by the big-bang nucleosynthesis [9], provided its mass is below a TeV. Since the right-chiral sneutrino has no gauge coupling but only interactions proportional to the neutrino Yukawa coupling, the strength of which is too feeble to be seen in dark matter search experiments, such a LSP is consistent with all direct

*sbiswas@hri.res.in

†biswarup@hri.res.in

¹It should be remembered that the above possibility is not unique. One may as well have a spectrum in which a third family squark is the NLSP [5,6].

searches carried out so far. Moreover, it has been shown that such a spectrum is consistent with all low-energy constraints [10], and the contribution to the relic density of the universe can be compatible with the limits set by the Wilkinson Microwave Anisotropy Probe [11] with appropriate values of the relevant parameters [12].

In this work, we have concentrated on the mass reconstruction of the lightest chargino in a $\tilde{\tau}$ -NLSP, $\tilde{\nu}_1$ -LSP scenario. This is a follow-up of our earlier work [13] on neutralino reconstruction under similar circumstances. We have shown that it is possible to determine the mass of the lightest chargino, produced in the cascade decay of squarks or gluinos, from the sharp drop noticed in the transverse mass [14] distribution of the chargino decay products. More precisely, we show a way of disentangling the transverse mass of the system consisting of a $\tilde{\tau}$ track and the associated neutrino from chargino decay. We suggest a method for extracting the transverse momentum (p_T) of the neutrino. Though a sizable statistics is required for this purpose, and one may have to wait for considerable accumulated luminosity after the discovery of the LHC, still this is a rather spectacular prospect. We have successfully applied the criteria, developed in our earlier work, for separating the signal from standard model backgrounds. Ways of suppressing SUSY processes that are likely to contaminate the transverse mass distributions are also suggested.

It should be mentioned that neither the signal we have studied nor the prescribed reconstruction technique is limited just to scenarios with right-sneutrino LSP. It can be applied successfully to all cases [15–17] where the NLSP is a charged scalar with quasistable character, provided that it decays outside the detector, leaving behind a charged track in the muon chamber.

The paper is organized as follows: in Sec. II, we motivate the scenario under investigation and present a brief review of the mass reconstruction for neutralinos as done in the earlier paper and used in this work. There we also summarize our choice of benchmark points (BPs). The signal under study and the reconstruction strategy for determining the chargino mass as well as the possible sources of background, both from the SM and within the model itself, and their possible discrimination, are discussed in Sec. III. We summarize and conclude in Sec. IV.

II. OVERALL SCENARIO, MASS RECONSTRUCTION, AND REPRESENTATIVE BENCHMARK POINTS

A. Scenarios with $\tilde{\nu}_R$ LSP and $\tilde{\tau}$ NLSP

As has been already stated, the most simpleminded extension of the MSSM [18], accommodating neutrino masses, is the addition of one right-handed neutrino superfield per family. In this situation the neutrinos have Dirac masses induced by very small Yukawa couplings. The superpotential of such an extended MSSM becomes (sup-

pressing family indices)

$$W_{\text{MSSM}} = y_l \hat{L} \hat{H}_d \hat{E}^c + y_d \hat{Q} \hat{H}_d \hat{D}^c + y_u \hat{Q} \hat{H}_u \hat{U}^c + \mu \hat{H}_d \hat{H}_u + y_\nu \hat{H}_u \hat{L} \hat{\nu}_R^c, \quad (1)$$

where \hat{H}_d and \hat{H}_u , respectively, are the Higgs superfields that give masses to the $T_3 = -1/2$ and $T_3 = +1/2$ fermions, and y 's are the strengths of Yukawa interaction. \hat{L} and \hat{Q} are the left-handed lepton and quark superfields, respectively, whereas \hat{E}^c , \hat{D}^c , and \hat{U}^c , in that order, are the right-handed gauge singlet charged lepton, down-type and up-type quark superfields. μ is the Higgsino mass parameter.

It is a common practice to attempt reduction of free parameters in the theory, by assuming a high-scale framework of SUSY breaking. The most commonly adopted scheme is based on $N = 1$ mSUGRA. There SUSY breaking in the hidden sector at high scale is manifested in universal soft masses for scalars (m_0) and gauginos ($M_{1/2}$), together with the trilinear (A) and bilinear (B) SUSY breaking parameters in the scalar sector. The bilinear parameter is determined by the electroweak symmetry breaking (EWSB) conditions. All the scalar and gaugino masses at low energy are obtained by renormalization group evolution of the universal mass parameters m_0 and $M_{1/2}$ from high-scale values [19]. Thus one generates all the squark, slepton, and gaugino masses as well as all the mass parameters in the Higgs sector. The Higgsino mass parameter μ (up to a sign), too, is determined from EWSB conditions. All one has to do in this scheme is to specify the high scale [$m_0, M_{1/2}, A_0$, together with $\text{sgn}(\mu)$ and $\tan\beta = \langle H_u \rangle / \langle H_d \rangle$], where $\tan\beta$ is the ratio of the vacuum expectation values of the two Higgs doublets that give masses to the up- and down-type quarks, respectively.

The neutrino masses are typically given by

$$m_\nu = y_\nu \langle H_u^0 \rangle = y_\nu v \sin\beta. \quad (2)$$

The small Dirac masses of the neutrinos imply that the neutrino Yukawa couplings (y_ν) are quite small ($\sim 10^{-13}$).

With the inclusion of the right-chiral neutrino superfields as a minimal extension, it makes sense to assume that the masses of their scalar components, too, originate in the same parameter m_0 . The evolution of all other parameters practically remains the same in this scenario as in the MSSM, while the right-chiral sneutrino mass parameter evolves at the one-loop level [20] as

$$\frac{dM_{\tilde{\nu}_R}^2}{dt} = \frac{2}{16\pi^2} y_\nu^2 A_\nu^2, \quad (3)$$

where A_ν is obtained by the running of the trilinear soft SUSY breaking term A and is responsible for left-right mixing in the sneutrino mass matrix.

It follows from above that the value of $M_{\tilde{\nu}_R}$ remains practically frozen at m_0 , thanks to the extremely small Yukawa couplings, whereas the other sfermion masses are enhanced at the electroweak scale. Thus, for a wide range of values of the gaugino masses, one naturally ends up with a sneutrino LSP ($\tilde{\nu}_1$), dominated by the right-chiral state. This is because the mixing angle is controlled by the neutrino Yukawa couplings:

$$\tilde{\nu}_1 = -\tilde{\nu}_L \sin\theta + \tilde{\nu}_R \cos\theta, \quad (4)$$

where the mixing angle θ is given by

$$\tan 2\theta = \frac{2y_\nu v \sin\beta |\cot\beta \mu - A_\nu|}{m_{\tilde{\nu}_L}^2 - m_{\tilde{\nu}_R}^2}. \quad (5)$$

Of the three charged sleptons, the amount of left-right mixing is always the largest in the third, and hence the lighter stau ($\tilde{\tau}_1$) often turns out to be the NLSP in such a scenario. There are regions in the parameter space where the three lighter sneutrino states corresponding to the three flavors act virtually as co-LSPs. It is, however, sufficient for illustrating our points to consider the lighter sneutrino mass eigenstate of the third family, as long as the state ($\tilde{\tau}_1$) is the lightest among the charged sleptons. Thus the addition of a right-handed sneutrino superfield, for each family, which is perhaps the most minimal input to explain neutrino masses and mixing, can eminently turn a mSUGRA theory into one with a stau NLSP and a sneutrino LSP. It should be emphasized that the physical LSP state can have (a) Yukawa couplings proportional to the neutrino mass and (b) gauge coupling with the small left-chiral admixture in it, driven by left-right mixing which is again proportional to y_ν . Thus the decay of any particle (particularly the NLSP) into the LSP will always be a very slow process, not taking place within the detector. Under such circumstances, the quintessential SUSY signal is not \cancel{E}_T anymore but a pair of charged tracks left by the quasistable NLSP.

B. Neutralino reconstructed

In an earlier study [13], we suggested a reconstruction technique for at least one of the two lightest neutralinos, in the $\tilde{\nu}_R$ -LSP and $\tilde{\tau}$ -NLSP scenario. The signal studied there was $2\tau_j + 2\tilde{\tau}$ (charged track) + $\cancel{E}_T + X$. Here τ_j denotes a jet out of one-prong decays of the τ , and all accompanying hard jets arising from cascades are included in X . The kinematic cuts imposed by us, such as $p_T^{\text{track}} > 100$ GeV and $\sum |\vec{p}_T| > 1$ TeV (p_T = transverse momentum, and $\sum |\vec{p}_T|$ is the scalar sum of all visible transverse momenta) reduced the backgrounds considerably.

Since the signal we investigated involves two τ 's in the final state, and hadronic decays of τ were considered, τ -jet identification and τ reconstruction were two important components of the procedure. For this a method suggested in [21] was used, which involved solving the following equation event by event:

$$\vec{p}_T = \left(\frac{1}{x_{\tau_{h1}}} - 1\right)\vec{p}_{h1} + \left(\frac{1}{x_{\tau_{h2}}} - 1\right)\vec{p}_{h2}, \quad (6)$$

where $x_{\tau_{hi}}$ ($i = 1, 2$) is the fraction of the τ energy carried by each product jet collinear with the parent τ , when it is boosted. \vec{p}_T is the vector sum of the transverse components of the 3-momenta of the two product neutrinos produced in hadronic decay of each τ . Clearly this method is applicable when there is no other invisible particle in the final state. This was ensured in the best possible manner by vetoing any isolated lepton in the final state, thus getting rid of additional neutrinos from W decays.

The reconstruction of \vec{p}_T is undoubtedly very crucial here. \vec{p}_T is reconstructed as the negative of the total visible \vec{p}_T which receives the contributions from isolated leptons/sleptons, jets, and unclustered components. The last among these includes all particles (electron/photon/ muon/stau) with $0.5 < E_T < 10$ GeV and $|\eta| < 5$ (for muon or muon-like tracks, $|\eta| < 2.5$), or hadrons with $0.5 < E_T < 20$ GeV and $|\eta| < 5$, which do not contribute to a jet and constitute ‘‘hits’’ in the detector [22]. In order to simulate the finite resolution of detectors, the energies/transverse momenta of all particles were smeared following prescriptions detailed in [13].

Once the τ 4-momenta are obtained, they are combined with the staus to find the stau- τ invariant mass distribution. This requires the knowledge of stau mass² as well as the choice of the correct pair. The correct pairs are obtained by using a seed mass for $\tilde{\tau}$ which was taken to be 100 GeV, satisfying the criterion $|M_{\tilde{\tau}\tau}^{\text{pair } 1} - M_{\tilde{\tau}\tau}^{\text{pair } 2}| < 50$ GeV. The actual stau mass is then extracted by demanding that the invariant masses of the two $\tilde{\tau}\tau$ pairs were equal, which yields an equation involving one unknown quantity, namely, $m_{\tilde{\tau}}$:

$$\begin{aligned} & \sqrt{m_{\tilde{\tau}}^2 + |\vec{p}_{\tilde{\tau}_1}|^2} \cdot E_{\tau_1} - \sqrt{m_{\tilde{\tau}}^2 + |\vec{p}_{\tilde{\tau}_2}|^2} \cdot E_{\tau_2} \\ & = \vec{p}_{\tilde{\tau}_1} \cdot \vec{p}_{\tau_1} - \vec{p}_{\tilde{\tau}_2} \cdot \vec{p}_{\tau_2}. \end{aligned} \quad (7)$$

Having thus extracted $m_{\tilde{\tau}}$ on an event-by-event basis in the event generator, it was demonstrated that the distribution of this mass value has a peak at the actual $m_{\tilde{\tau}}$. We have used this peak value in reconstructing the neutralino from the invariant mass distribution of the $\tilde{\tau}\tau$ pair. In some regions of the parameter space, it is possible to thus reconstruct only χ_1^0 , as the production rate of χ_2^0 in cascade decay of \tilde{q} (or \tilde{g}) as well as the decay branching ratio of $\chi_2^0 \rightarrow \tilde{\tau}\tau$ is small. In some other regions, we have been able to reconstruct both of them. There are still other regions where only the χ_2^0 peak shows up. This is because of the small mass splitting between χ_1^0 and $\tilde{\tau}$, which softens

²From the muon chamber only the three-momenta of the charged track can be obtained.

TABLE I. Proposed benchmark points (BP) for the study of the stau-NLSP scenario in SUGRA with right-sneutrino LSP. The values of m_0 and $M_{1/2}$ are given in GeV. We have also set $A_0 = 100$ GeV and $\text{sgn}(\mu) = +$ for benchmark points under study.

	BP1	BP2	BP3	BP4	BP5	BP6
	$m_0 = 100$	$m_0 = 100$	$m_0 = 100$	$m_0 = 100$	$m_0 = 100$	$m_0 = 100$
	$m_{1/2} = 600$	$m_{1/2} = 500$	$m_{1/2} = 400$	$m_{1/2} = 350$	$m_{1/2} = 325$	$m_{1/2} = 325$
mSUGRA input	$\tan\beta = 30$	$\tan\beta = 30$	$\tan\beta = 30$	$\tan\beta = 30$	$\tan\beta = 30$	$\tan\beta = 25$
$m_{\tilde{e}_L}, m_{\tilde{\mu}_L}$	418	355	292	262	247	247
$m_{\tilde{e}_R}, m_{\tilde{\mu}_R}$	246	214	183	169	162	162
$m_{\tilde{\nu}_{eL}}, m_{\tilde{\nu}_{\mu L}}$	408	343	279	247	232	232
$m_{\tilde{\nu}_{eL}}$	395	333	270	239	224	226
$m_{\tilde{\nu}_{iR}}$	100	100	100	100	100	100
$m_{\tilde{\tau}_1}$	189	158	127	112	106	124
$m_{\tilde{\tau}_2}$	419	359	301	273	259	255
$m_{\chi_1^0}$	248	204	161	140	129	129
$m_{\chi_2^0}$	469	386	303	261	241	240
$m_{\chi_1^\pm}$	470	387	303	262	241	241
$m_{\tilde{g}}$	1362	1151	937	829	774	774
$m_{\tilde{t}_1}$	969	816	772	582	634	543
$m_{\tilde{t}_2}$	1179	1008	818	750	683	709
m_{h^0}	115	114	112	111	111	111

the τ (jet) arising from its decay, preventing it from passing the requisite hardness cut.

C. Choice of benchmark points

The choice of benchmark points for this study is the same as in the case of neutralino reconstruction [13]. The mSUGRA parameter space is utilized for this purpose. A $\tilde{\tau}$ NLSP and a $\tilde{\nu}_1$ LSP occur in those regions in which one would have had a $\tilde{\tau}$ LSP in the absence of right-chiral neutrino superfields. We focus on both the regions where (a) $m_{\tilde{\tau}_1} > m_{\tilde{\nu}_1} + m_W$ and (b) the above inequality is not satisfied. In the first case, the dominant decay mode is the two-body decay of the NLSP, $\tilde{\tau}_1 \rightarrow \tilde{\nu}_1 W$, and, in the second, the decay takes place via a virtual W . Decay into a charged Higgs is a subdominant channel for the lighter stau. The decay takes place outside the detector in all cases. At different benchmark points, however, the mass splittings between the $\tilde{\tau}_1$ and neutralinos/charginos are different. This in turn affects the kinematic characteristics of the final states under consideration.

We have used the spectrum generator ISAJET 7.78 [23] for our study. In Table I we list the six benchmark points used, both in terms of high-scale parameters and low-energy spectra. The justification of their choice and their representative character have been explained in Ref. [13].

It may be noted that the region of the mSUGRA parameter space where we have worked is consistent with all the experimental bounds [24], including both collider and low-energy constraints [such as the LEP and Tevatron constraints on the masses of Higgs, gluinos, charginos, etc., as also those from $b \rightarrow s\gamma$, correction to the ρ parameter, $(g_\mu - 2)$, and so on]. In the next section we

describe the procedure for the reconstruction of χ_1^\pm for these benchmark points.

III. RECONSTRUCTION OF THE LIGHTER CHARGINO

The final state of use for the reconstruction of the lighter chargino is

$$\tau_j + 2\tilde{\tau}(\text{opposite-sign charged tracks}) + \cancel{E}_T + X,$$

where τ_j represents a jet which has been identified as a τ jet, the missing transverse energy is denoted by \cancel{E}_T , and all other jets coming from cascade decays are included in X .³

Simulation for the LHC has been done for the signal as well as backgrounds using PYTHIA (v6.4.16) [25]. The pp events have been studied with a center-of-mass energy ($E_{\text{c.m.}}$) = 14 TeV at an integrated luminosity of 300 fb^{-1} . The numerical values of the electromagnetic and the strong coupling constant have been set at $\alpha_{\text{em}}^{-1}(M_Z) = 127.9$ and $\alpha_s(M_Z) = 0.118$, respectively [10]. The hard scattering process has been folded with CTEQ5L parton distribution function [26]. We have set the factorization and renormalization scales at the average mass of the particles produced in the parton level hard scattering process. In order to make our estimate conservative, the signal rates have not been multiplied by any K factor [27]. The effects of initial and final state radiation as well as the finite detector resolution of the energies/momenta of the final state particles have been taken into account.

³In order to avoid the combinatorial backgrounds, we have considered events with two opposite sign $\tilde{\tau}$'s only.

A. Chargino reconstruction from transverse mass distribution

Now we are all set to describe the main principle adopted by us for chargino (χ_1^\pm) reconstruction. For this purpose, we have looked for the processes in which $\chi_1^\pm - \chi_1^0/\chi_2^0$ is being produced in association with hard jets in cascade decays of squarks and gluinos. The χ_1^\pm subsequently decays into a $\tilde{\tau}-\nu_\tau$ pair, while the χ_1^0 (or χ_2^0) decays into a $\tilde{\tau}-\tau$ pair. Since the decay of χ_1^\pm involves an invisible particle (ν_τ), for which it is not possible to know all the four components of momenta, a transverse mass distribution, rather than invariant mass distribution, of $\tilde{\tau}-\nu_\tau$ pair will give us mass information of χ_1^\pm . In spite of the recent progress in measuring the masses of particles in semi-invisible decay mode (for example, the m_{T_2} variable introduced by [28] and its further implications [29]), we have focused on transverse mass variable (m_T) because of the fact that the only invisible particle present in the final state is the neutrino, which is massless.

The procedure, however, still remains problematic, because the τ on the other side (arising from neutralino decay) also produces a neutrino in the final state, which contributes to \cancel{E}_T . In order to correctly reconstruct the transverse mass of the $\tilde{\tau}-\nu_\tau$ pair from chargino decay, the contribution to \cancel{E}_T from the aforementioned neutrino must be subtracted.

Keeping this in mind, we have prescribed a method for reconstruction of the transverse component of the neutrino 4-momenta ($\vec{P}_{\nu_1}^T$) produced from the decay of χ_1^\pm , in association with $\tilde{\tau}$. To describe it in short:

We label the transverse momentum of the neutrino coming from chargino decay by $\vec{P}_{\nu_1}^T$. Attention is focused on cases where the τ , produced from a neutralino, decays hadronically and the τ jet, out of a one-prong decay of τ , is identified following the prescription of [21]. We have assumed a true τ -jet identification efficiency to be 50%, while a non- τ jet rejection factor of 100 has been used [30–32] (The results for higher identification efficiency are also shown in Sec. IV.) We have also assumed that there is no invisible particle other than the two neutrinos mentioned above. We have attempted to ensure this by vetoing any event with isolated charged leptons. This only leaves out neutrinos from Z -decay and W decays into a $\tau\nu_\tau$ pair. The contamination of our signal from these are found to be rather modest.

The transverse momenta of the neutrino ($\vec{P}_{\nu_2}^T$), out of a τ decay, is first reconstructed in the collinear approximation, where the product neutrino and the jet are both assumed to move collinearly with the parent τ . In this approximation, one can write

$$P_{\tau_j} = xP_\tau. \quad (8)$$

Following the decay χ_1^0 (or χ_2^0) $\rightarrow \tilde{\tau}^\pm \tau^\mp$ we have then combined the identified τ jet with the oppositely charged

stau (track), thus forming the invariant mass

$$m_{\chi_i^0}^2 = (P_{\tilde{\tau}} + P_\tau)^2 = (P_{\tilde{\tau}} + P_{\tau_j}/x)^2 \quad (i = 1, 2). \quad (9)$$

This pairing requires the charge information of the τ -induced jet. We have assumed that, for a true τ jet, the charge identification efficiency is 100%, while to a non- τ jet we have randomly assigned positive and negative charge, each with 50% weight. One can solve this equation for x (neglecting the τ -jet invariant mass⁴), to obtain

$$x \approx \frac{2P_{\tilde{\tau}} \cdot P_{\tau_j}}{m_{\chi_i^0}^2 - m_{\tilde{\tau}}^2}. \quad (10)$$

This requires the information of $m_{\chi_1^0}$ (or $m_{\chi_2^0}$) and $m_{\tilde{\tau}}$ as well, which we have used from our earlier work for the respective benchmark points. Once x is known, we have

$$\vec{P}_{\nu_2}^T = \vec{P}_\tau^T - \vec{P}_{\tau_j}^T = \frac{1-x}{x} \cdot \vec{P}_{\tau_j}^T. \quad (11)$$

Hence, the transverse component of the neutrino, out of χ_1^\pm decay, can be extracted from the knowledge of $\vec{\cancel{E}}_T$ of that particular event.⁵ This is given by

$$\vec{P}_{\nu_1}^T = \vec{\cancel{E}}_T - \vec{P}_{\nu_2}^T. \quad (12)$$

Finally, from the end point of the transverse mass distribution of the $\tilde{\tau}-\nu_\tau$ pair the value of $m_{\chi_1^\pm}$ can be obtained. However, one should keep in mind that both χ_1^0 and χ_2^0 can decay into a $\tilde{\tau}\tau$ pair. Therefore, it is necessary to specify some criterion to separate whether a given $\tilde{\tau}\tau$ pair has originated from a χ_1^0 or χ_2^0 , which we will discuss in the next subsection.

B. Distinguishing between decay products of χ_1^0 and χ_2^0

In order to identify the origin of a given opposite sign $\tilde{\tau}-\tau$ pair, the first information that is to be extracted from the data is which benchmark region one is in. We have assumed gaugino mass universality for this process, for the sake of simplicity.

If one looks at the effective mass (defined by $M_{\text{eff}} = \sum |\vec{p}_T| + \vec{\cancel{E}}_T$) distribution of the final state, then the peak of the distribution gives one an idea of the masses of the strongly interacting superparticles which are the dominant products of the initial hard scattering process. This is seen from Fig. 1. Once the order of magnitude of the gluino mass is inferred from this distribution, one can use the universality of gaugino masses, which, in turn, indicates where $m_{\chi_1^0}$ and $m_{\chi_2^0}$, masses of the two lightest neutralinos, are expected to lie.

⁴This approximation is not valid for small x , say, $x < 0.1$. However, the jet out of a τ decay almost always carries a larger fraction of τ energy, thus justifying the approximation.

⁵For details on the reconstruction of $\vec{\cancel{E}}_T$, see [13].

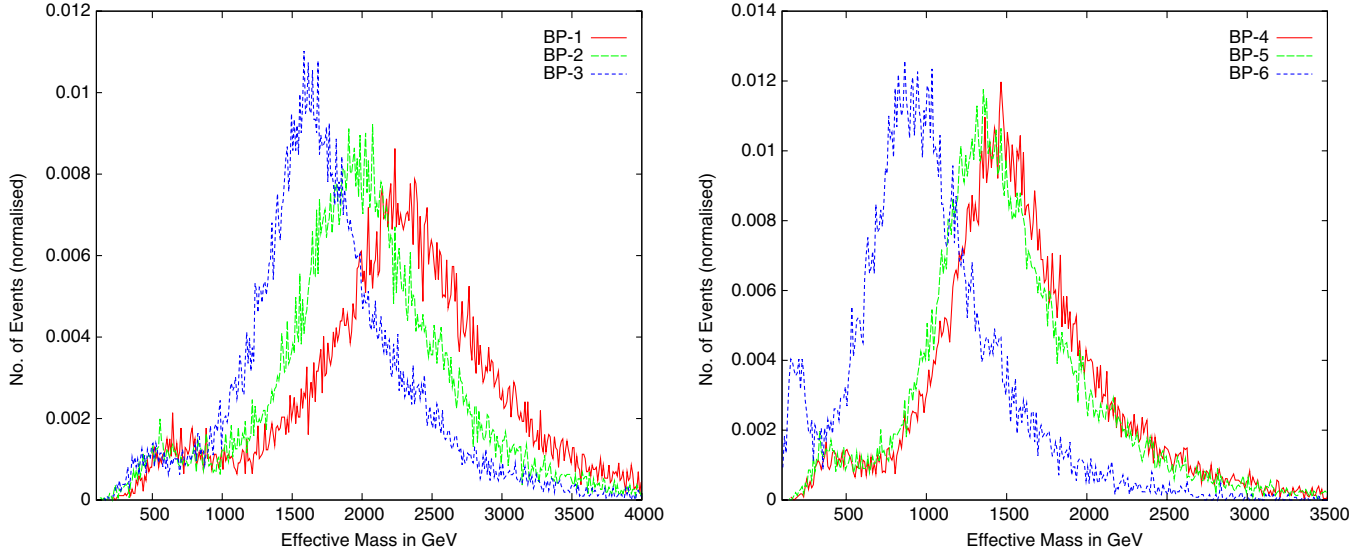


FIG. 1 (color online). M_{eff} distribution (normalized to unity) of the final state under consideration, for all benchmark points.

Next, for each event that we record, we look at a $\tilde{\tau}$ and a τ jet of opposite signs. The invariant mass distribution of this $\tilde{\tau}\tau_j$ pair displays a peak whose location, although not precisely telling us about the parent neutralino, is still in the vicinity of the mass values. Thus, by observing these distributions (Fig. 2) one often is able to tell whether it is a χ_1^0 or a χ_2^0 , once one simultaneously uses information obtained from the M_{eff} distribution.

As has already been noted in [13], the mass of either χ_1^0 or χ_2^0 or both can be reconstructed in this scenario, depending on one's location in the parameter space. Once a peak in the $\tau\tilde{\tau}$ invariant mass is located, the next step is to check whether $|M_{\tilde{\tau}-\tau_j} - m_{\chi_i^0}| < 0.1 \cdot m_{\chi_i^0}$, where $m_{\chi_i^0}$ is either one (or the only one) of the two lightest neutralinos deemed reconstructible in the corresponding region. The mass of that neutralino is used in Eq. (9). If this equality is not satisfied for either neutralino or the only one reconstructed, then the event is not included in the analysis.

C. SM backgrounds and cuts

The final state we have considered, namely, $\tau_j + 2\tilde{\tau}$ (opposite-sign charged track) + $\cancel{E}_T + X$, suffers from several SM background processes. This is because charged tracks in the muon chamber due to the presence of quasi-stable charged particle can be faked by muons. Such faking is particularly likely for ultrarelativistic particles, for which neither the time-delay measurement nor the degree of ionization in the inner tracking chamber is a reliable discriminator. The dominant contributions come from the following subprocesses:

- (1) $t\bar{t}$: This is a potential background for any final state in the context of LHC, due to its large production cross section. In this case $t\bar{t} \rightarrow bW^+ \bar{b}W^-$, followed

by various combinations of leptonic as well as hadronic decays of the b and the W , can produce opposite sign dimuons and jets. The jets may emanate from actual τ 's, but may as well be fake. One has an efficiency of 50% in the former case, and a mistagging probability of 1% in the latter. The $t\bar{t}$ cross section has been multiplied by a K factor of 1.8 [33].

- (2) $b\bar{b}$: This, too, has an overwhelmingly large event rate at the LHC. The semileptonic decay of both the b 's ($b \rightarrow c\mu\nu_\mu$) can give rise to a dimuon final state and any of the associated jets can be faked as τ jet. Though the mistagging probability of a non- τ jet being identified as a τ jet is small, the large cross section of $b\bar{b}$ production warrants serious attention to this background.
- (3) ZZ : In this case any one of the Z 's can decay into a dimuon pair ($Z \rightarrow \mu\mu$) while the other one can decay into $\tau\tau$ pair where only one of the τ can be identified. The hadronic decay of Z and the subsequent misidentification of any of them as τ jet is also possible.
- (4) ZW : This SM process also contributes to the final state under consideration with $Z \rightarrow \mu\mu$ and $W \rightarrow \tau\bar{\nu}_\tau$.
- (5) ZH : This subprocess can also contribute to the final state $\tau_j + 2\mu$ (charged track) + \cancel{E}_T where the Higgs decaying into a pair of τ 's, with only one of the τ being identified has been considered.

Our chosen event selection criteria have been prompted by all the above backgrounds. First of all, we have subjected the events to the following basic cuts:

- (i) $p_T^{\text{lep, track}} > 10 \text{ GeV}$
- (ii) $p_T^{\text{hardest jet}} > 75 \text{ GeV}$

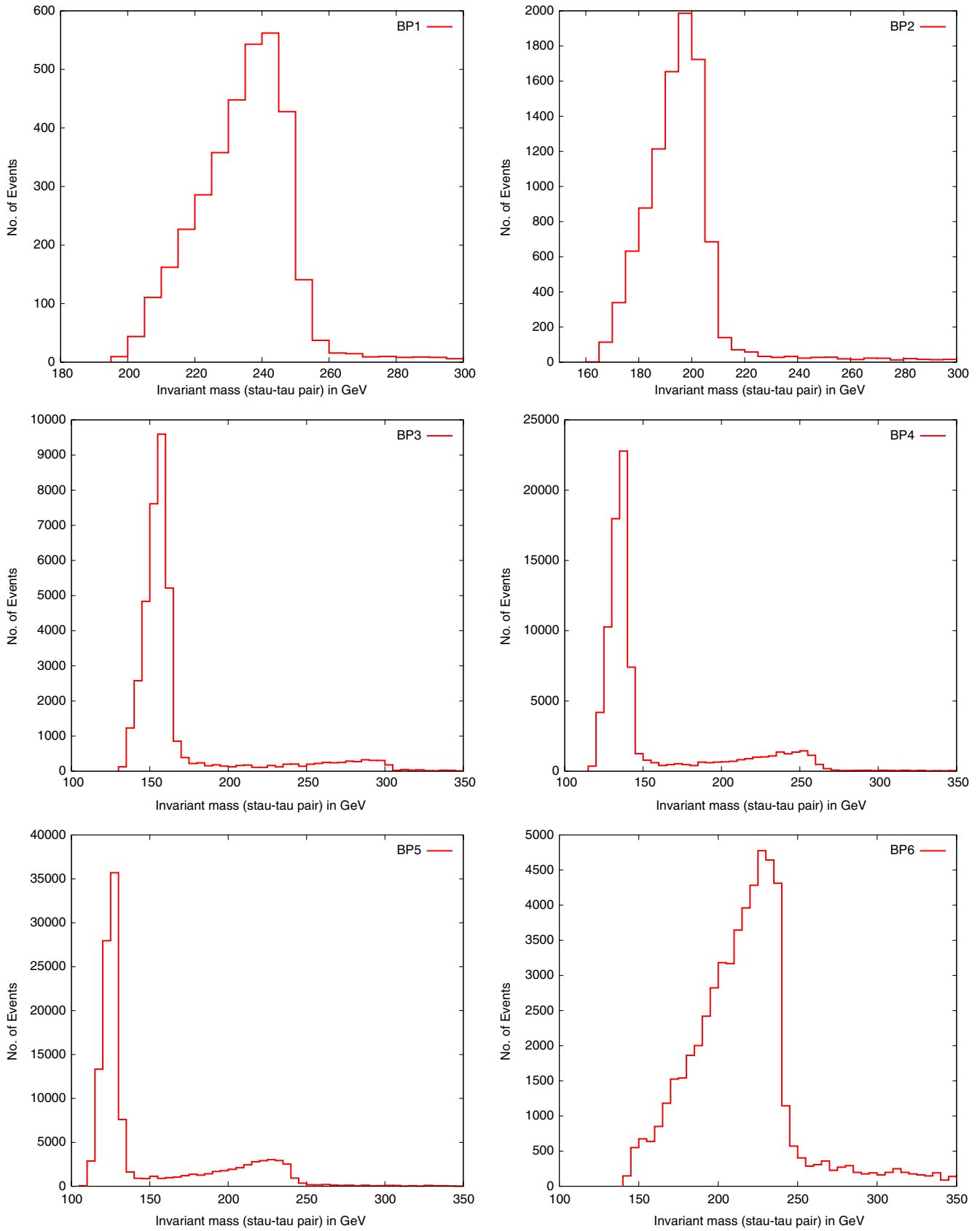


FIG. 2 (color online). $M_{\tilde{\tau}\tau_j}$ distribution for all the benchmark points. BP1, BP2, and BP3 show only the χ_1^0 peak. Both the χ_1^0 and χ_2^0 peaks are visible for BP4 and BP5, while BP6 displays only the χ_2^0 peak.

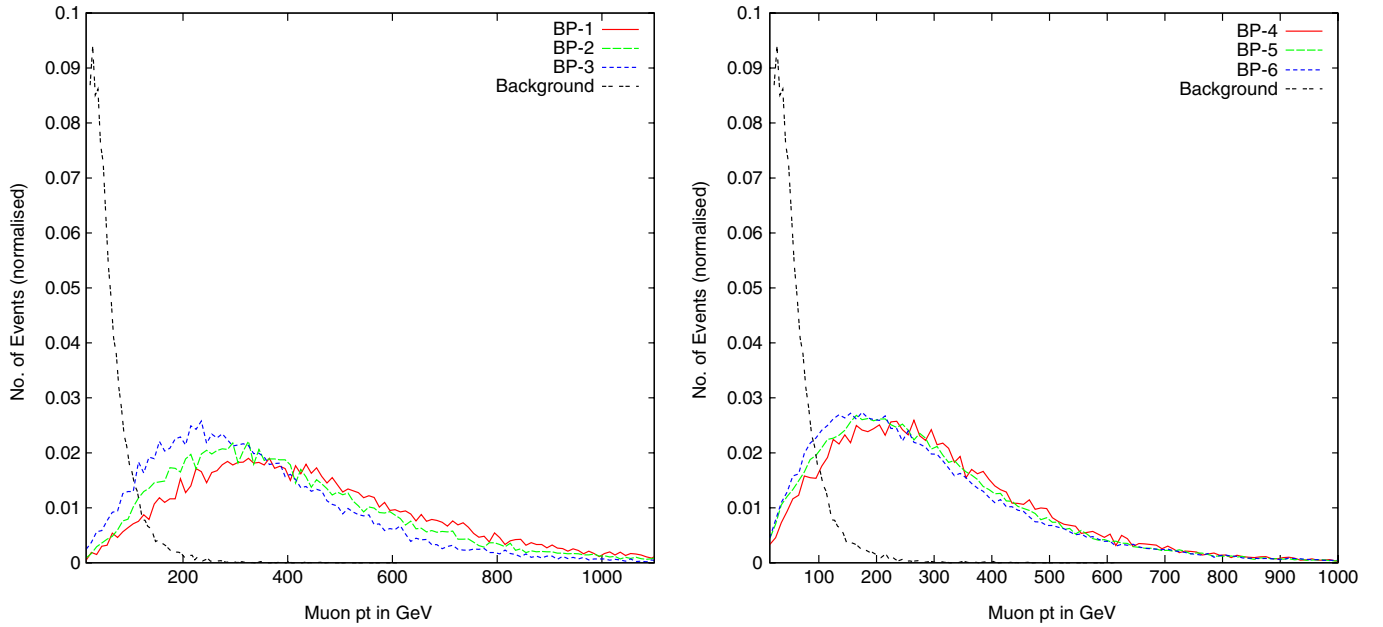


FIG. 3 (color online). p_T distribution (normalized to unity) of the harder muonlike track for the signal and the background, for all benchmark points. The vertical lines indicate the effects of a p_T cut at 100 GeV.

- (iii) $p_T^{\text{other jets}} > 30 \text{ GeV}$
- (iv) $40 < \cancel{E}_T < 180 \text{ GeV}$
- (v) $|\eta| < 2.5$ for leptons, jets, and stau
- (vi) $\Delta R_{ll} > 0.2$, $\Delta R_{lj} > 0.4$, where $\Delta R^2 = \Delta\eta^2 + \Delta\phi^2$
- (vii) $\Delta R_{\tilde{\tau}l} > 0.2$, $\Delta R_{\tilde{\tau}j} > 0.4$
- (viii) $\Delta R_{jj} > 0.7$

Though the above cuts largely establish the genuineness of

a signal event, the background events are too numerous to be effectively suppressed by them. One therefore has to use the fact that the jets and stau tracks are all arising from the decays of substantially heavy sparticles. This endows them with added degrees of hardness, as compound to jets and muons produced in SM process. Thus we can impose a p_T cut on each track on the muon chamber, and also demand a large value of the scalar sum of transverse momenta of all the visible final state particles:

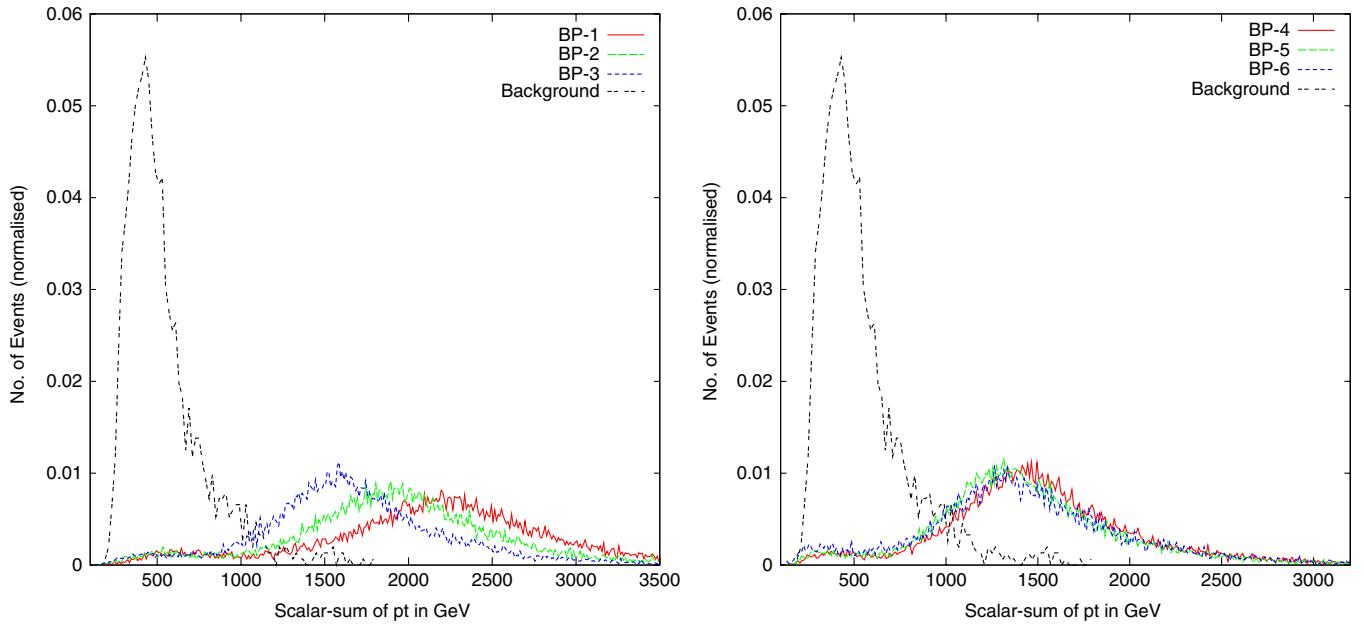


FIG. 4 (color online). $\sum |p_T|$ distribution (normalized to unity) for the signal and the background, for all benchmark points.

- (i) $p_T^{\text{muonlike track}} > 100 \text{ GeV}$
- (ii) $\sum |\vec{p}_T| > 1 \text{ TeV}$

The justification of these cuts can also be seen from Figs. 3 and 4. It may be noted that no invariant mass cut on the pair of charged tracks has been imposed. While such a cut, too, can suppress the dimuon background, we find it more rewarding to use the scalar sum of p_T cut.

D. SUSY backgrounds

Apart from the SM backgrounds, SUSY processes in this scenario itself contribute to the final state $\tau_j + 2\tilde{\tau} + \cancel{E}_T + X$, which are often more serious than the SM backgrounds. These events will survive the kinematic cuts listed in the previous subsection, since they, too, originate in heavy sparticles produced in the initial hard scattering. The dominant contributions of this kind come from:

- (1) $\chi_i^0 \chi_j^0$ production in cascade decay of squarks/gluinos: This is one of the potentially dangerous backgrounds where both the χ_i^0 's ($i, j = 1, 2$) decay into $\tilde{\tau}\tau$ pairs, with only one τ being identified. This then mimics our final state in all details with a much higher event rate.
- (2) $\tilde{\nu}_{\tau_L} \chi_i^0$ production in cascade decay of squarks/gluinos: The decay of $\tilde{\nu}_{\tau_L}$ as part of the cascade produces a $W\tilde{\tau}_1$ pair, while the χ_i^0 decays into a $\tilde{\tau}\tau$ pair to give rise to the same final state with an additional

W which then can decay hadronically. The $\tilde{\nu}_{\tau_L}$ is produced in association with a τ in a large number of events (e.g., $\chi_1^\pm \rightarrow \tilde{\nu}_{\tau_L}\tau$). The $\tilde{\nu}_{\tau_L}$ can also be produced from, say, a χ_2^0 . In both of the above situations, a τ -stau pair can be seen together with another stau track, thus leading to a background event.

The first background can be reduced partially by looking at the invariant mass distribution of the $\tilde{\tau}$ (having the same sign as that of the *identified* τ in the final state) with each jet in the final state. If this distribution for any particular combinations falls within $m_{\chi_i} - 20 < M_{\tilde{\tau}j} < m_{\chi_i} + 20$ (where $m_{\chi_i} = m_{\chi_1^0}$ or $m_{\chi_2^0}/2$, depending on whether χ_1^0 or χ_2^0 is better constructed), we have thrown away that event. The reason for this lies in the observations depicted in Fig. 2: the invariant mass of a τ -induced jet and the $\tilde{\tau}$ which shows a peak close to the mass of the neutralino from which the $\tilde{\tau}$ - τ pair is produced. This has been denoted by cut X in Tables II and III. In addition, if the available information on the effective mass tells us that the χ_2^0 is better reconstructed in the region, and is produced along with a χ_1^0 with substantial rate, then a similar invariant mass cut around the χ_2^0 mass will also be useful. A further cut on the transverse mass distribution $M_{\tilde{\tau}\nu_\tau}^T (> 1.5m_{\chi_1^0}$ or $0.75m_{\chi_2^0})$ substantially decreases this background without seriously affecting the signal.

TABLE II. Number of signal and background events for the $\tau_j + 2\tilde{\tau}$ (charged track) + $\cancel{E}_T + X$ final state, considering all SUSY processes, for BP1, BP2, and BP3 at an integrated luminosity 300 fb^{-1} assuming τ -identification efficiency $\epsilon_\tau = 50\%$.

BP1	Signal ($\chi_{1/2}^0 - \chi_1^\pm$)	SM backgrounds	$\chi_1^0 - \chi_1^0$	SUSY backgrounds		
				$\chi_1^0 - \chi_2^0$	$\chi_2^0 - \chi_2^0$	$\chi_{1/2}^0 - \tilde{\nu}_{\tau_L}$
Basic cuts	121	65 588	2557	62	1	786
With $p_T + \sum p_T $ cut	92	202	2236	49	1	551
Cut Y	83	202	1969	42	1	433
Cut X	58	202	1130	26	1	244
$M_{\tilde{\tau}\nu_\tau}^T > \frac{3}{4}m_{\chi_2^0}$	28	0	83	2	0	25
$ M_{\text{peak}} - M_{\tilde{\tau}\nu_\tau}^T \leq 20$	9	0	7	0	0	2
BP2	Signal ($\chi_{1/2}^0 - \chi_1^\pm$)	SM backgrounds	$\chi_1^0 - \chi_1^0$	SUSY backgrounds		
Basic cuts	677	65 588	6600	$\chi_1^0 - \chi_2^0$	$\chi_2^0 - \chi_2^0$	$\chi_{1/2}^0 - \tilde{\nu}_{\tau_L}$
With $p_T + \sum p_T $ cut	492	202	5552	390	9	2157
Cut Y	444	202	4885	301	7	1418
Cut X	336	202	2675	262	6	1106
$M_{\tilde{\tau}\nu_\tau}^T > \frac{3}{4}m_{\chi_2^0}$	173	0	278	170	5	605
$ M_{\text{peak}} - M_{\tilde{\tau}\nu_\tau}^T \leq 20$	62	0	33	26	1	76
				5	0	11
BP3	Signal ($\chi_{1/2}^0 - \chi_1^\pm$)	SM backgrounds	$\chi_1^0 - \chi_1^0$	SUSY backgrounds		
Basic cuts	5519	65 588	19 400	$\chi_1^0 - \chi_2^0$	$\chi_2^0 - \chi_2^0$	$\chi_{1/2}^0 - \tilde{\nu}_{\tau_L}$
With $p_T + \sum p_T $ cut	3571	202	15 181	3361	170	6959
Cut Y	3131	202	13091	2240	98	4186
Cut X	2372	202	6974	1924	91	3231
$M_{\tilde{\tau}\nu_\tau}^T > \frac{3}{4}m_{\chi_2^0}$	1189	0	985	1192	71	1679
$ M_{\text{peak}} - M_{\tilde{\tau}\nu_\tau}^T \leq 20$	523	0	154	205	14	208
				46	1	27

TABLE III. Same as in Table II, but for BP4, BP5, and BP6.

BP4	Signal ($\chi_{1/2}^0 - \chi_1^\pm$)	SM backgrounds	$\chi_1^0 - \chi_1^0$	SUSY backgrounds		
				$\chi_1^0 - \chi_2^0$	$\chi_2^0 - \chi_2^0$	$\chi_{1/2}^0 - \tilde{\nu}_{\tau L}$
Basic cuts	18 194	65 588	33 076	10 618	886	10 613
With $p_T + \Sigma p_T $ cut	10 697	202	24 475	6342	439	5713
Cut Y	9431	202	21100	5431	368	4436
Cut X	4875	202	7583	2132	157	1480
$M_{\tilde{\nu}\nu_\tau}^T > \frac{3}{4}m_{\chi_2^0}$	2345	0	1274	439	41	231
$ M_{\text{peak}} - M_{\tilde{\nu}\nu_\tau}^T \leq 20$	1076	0	254	114	13	58
				SUSY backgrounds		
BP5	Signal ($\chi_{1/2}^0 - \chi_1^\pm$)	SM backgrounds	$\chi_1^0 - \chi_1^0$	$\chi_1^0 - \chi_2^0$	$\chi_2^0 - \chi_2^0$	$\chi_{1/2}^0 - \tilde{\nu}_{\tau L}$
Basic cuts	34 489	65 588	39 521	19 574	1976	12 039
With $p_T + \Sigma p_T $ cut	18 748	202	28 329	10 827	958	5953
Cut Y	16 419	202	24 348	9326	815	4586
Cut X	8508	186	8869	3764	376	1626
$M_{\tilde{\nu}\nu_\tau}^T > \frac{3}{4}m_{\chi_2^0}$	4099	0	1574	866	144	258
$ M_{\text{peak}} - M_{\tilde{\nu}\nu_\tau}^T \leq 20$	2145	0	339	221	52	37
				SUSY backgrounds		
BP6	Signal ($\chi_{1/2}^0 - \chi_1^\pm$)	SM backgrounds	$\chi_1^0 - \chi_1^0$	$\chi_1^0 - \chi_2^0$	$\chi_2^0 - \chi_2^0$	$\chi_{1/2}^0 - \tilde{\nu}_{\tau L}$
Basic cuts	17 146	65 588	14 519	20 756	1970	4644
With $p_T + \Sigma p_T $ cut	8379	202	9593	11 405	968	2524
Cut Y	7326	202	8004	9776	778	2025
Cut X	4204	186	3837	5697	374	1038
$M_{\tilde{\nu}\nu_\tau}^T > \frac{3}{4}m_{\chi_2^0}$	1475	0	231	1783	128	15
$ M_{\text{peak}} - M_{\tilde{\nu}\nu_\tau}^T \leq 20$	774	0	62	569	44	0

The background of the second kind can in principle be reduced by vetoing events with additional W 's. To identify events with W we have considered only the hadronic decays of W 's. We first observe the ΔR separation between the stau (produced in decay of $\tilde{\nu}_{\tau L}$) and the direction formed out of the vector sum of the momenta of the two jets produced in W decay. If this separation lies within $\Delta R = 0.8$ and the invariant mass of the two jets lies within $M_W - 20 < M_{jj} < M_W + 20$ we discard that particular event. In addition, for a sufficiently boosted W , one can have a situation where the two jets merge to form a single jet. For such a case, we again look at the stau and each jet within $\Delta R < 0.8$ around it. The invariant mass of the resultant jet is taken to be 20% of the jet energy. The event is rejected if a jet with the mass lies within ± 20 GeV of the W mass. We have denoted this by cut Y in Tables II and III. Of course, while it is useful in reducing the background, a fraction of the signal events also gets discarded in the process.

IV. NUMERICAL RESULTS

We finally present the numerical results of our study, after imposing the various cuts for all the benchmark points. From Tables II and III one can see that, after demanding a minimum hardness of the charged track

($p_T^{\text{track}} > 100$ GeV), together with the cut on the scalar sum of p_T ($\Sigma|p_T| > 1$ TeV), the contribution from the SM processes gets reduced substantially. The cuts X and Y , defined in the previous subsection, are relatively inconsequential for SM processes. However, in the process of solving for neutrino momentum in τ decay, most of the SM background events get eliminated on demanding the invariant mass of the τ , paired with an oppositely charged track, to be around the neutralino mass ($m_{\chi_1^0}$ or $m_{\chi_2^0}$). This is due to the demand that the solution be physical, i.e., the fraction x lies between 0 and 1. It is very unlikely to have admissible solutions for x in SM processes, with the τ -(muon) track pair invariant mass peaking at $m_{\chi_1^0}/m_{\chi_2^0}$. Thus, although the demand $0 < x < 1$ is not meant specifically for background elimination, it is nonetheless helpful in reducing backgrounds. We have verified that the SM contributions within a bin of ± 20 GeV around the reconstructed peak are very small.

As has been already mentioned, SUSY backgrounds within the model itself are hard to get rid of completely. The peak in the transverse mass distribution of the $\tilde{\tau}\nu_\tau$ pair gets smeared due to such background events (see Fig. 4). We have already mentioned two suggested cuts, namely, X and Y , which partially reduce these backgrounds. Of these, cut Y suppresses (by about 15%) some

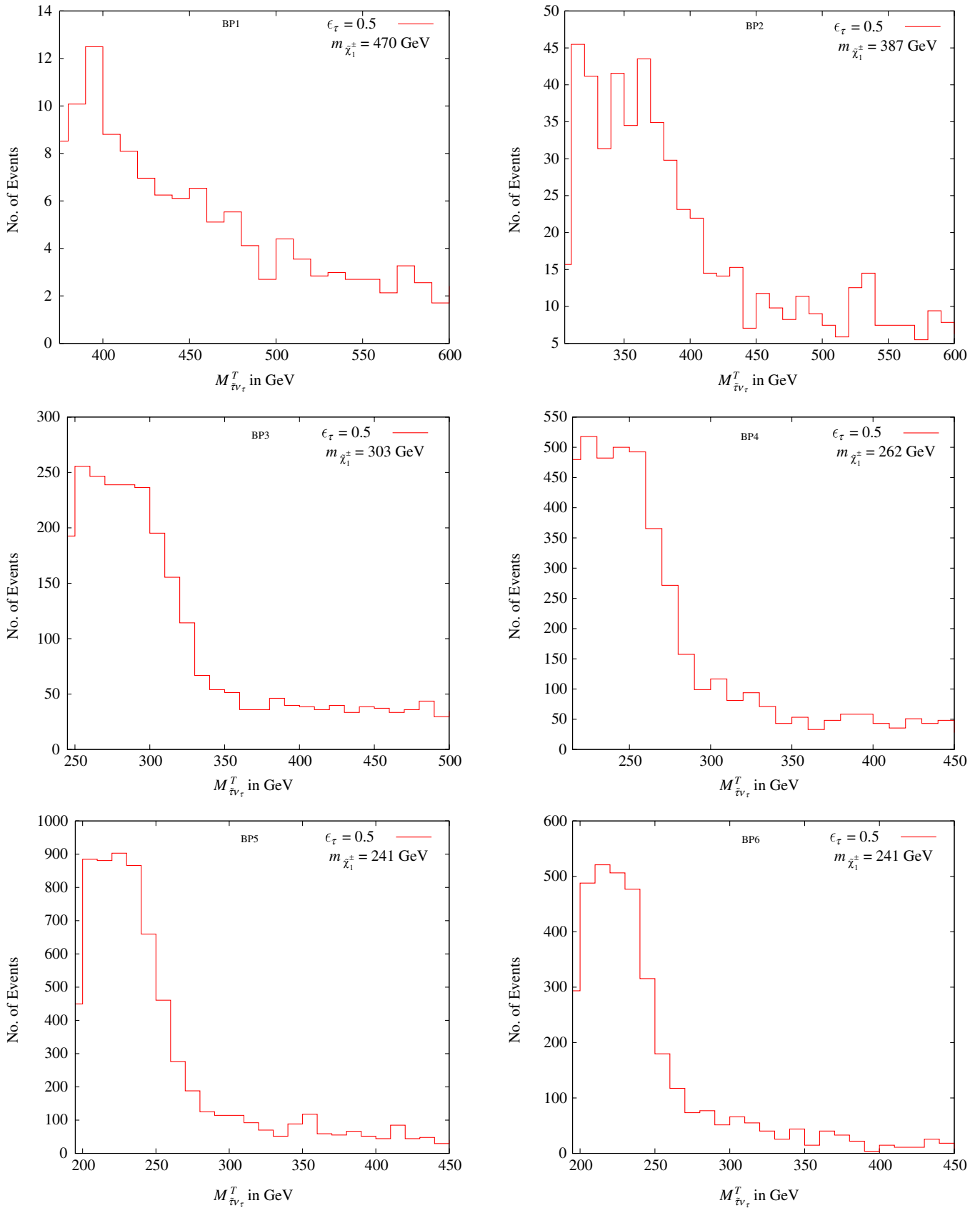


FIG. 5 (color online). The transverse mass $\tilde{\tau}\nu_\tau$ pair from chargino decay described in the text, for all the benchmark points with τ -identification efficiency (ϵ_τ) = 50%.

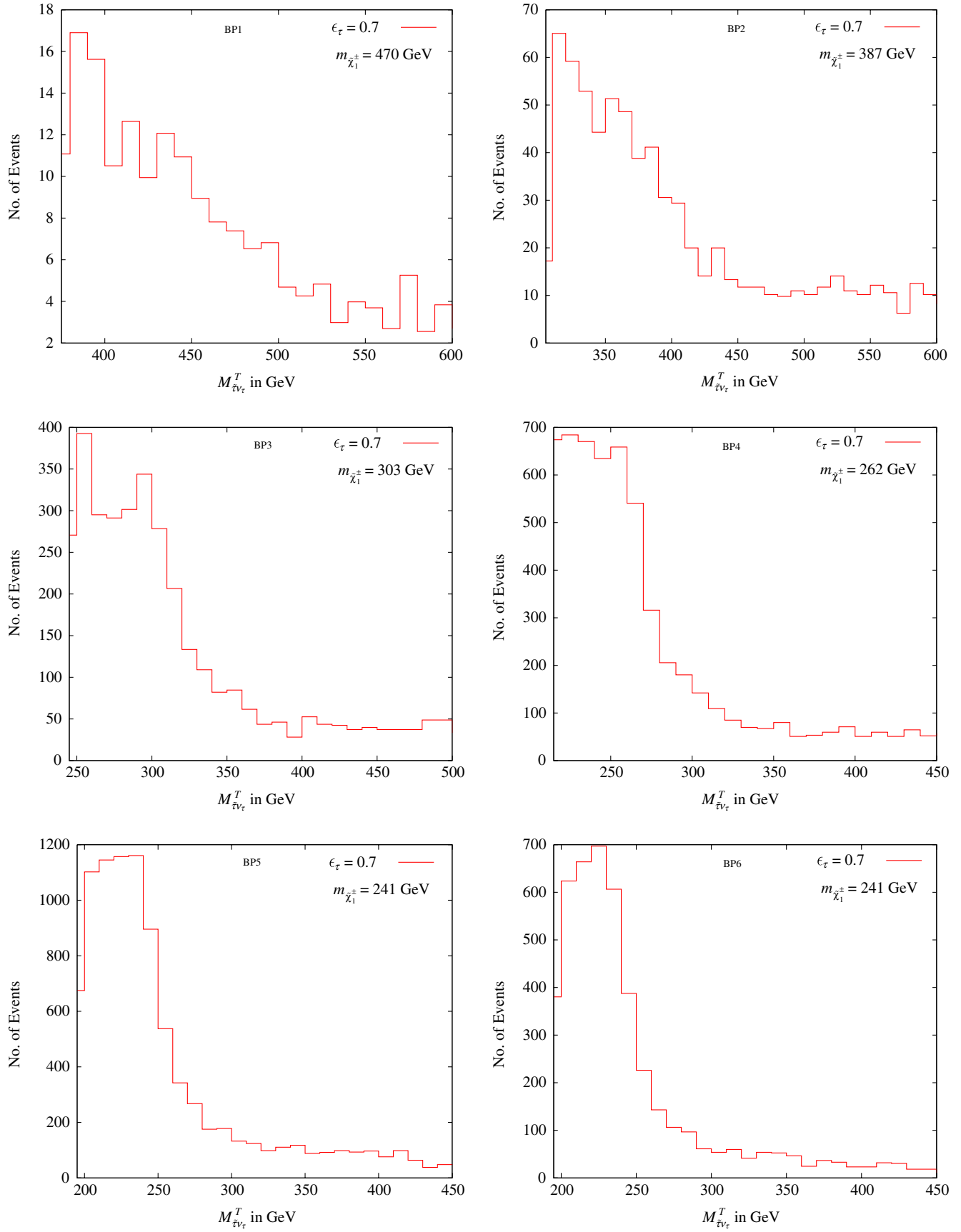


FIG. 6 (color online). Same as in Fig. 5, but with τ -identification efficiency (ϵ_τ) = 70%.

of the $\tilde{\nu}_{\tau_L}\text{-}\chi_{1/2}^0$ events, as can be seen from Tables II and III. The effects of this cut on the other SUSY backgrounds as well as the signal are very similar.

Cut X is meant to eliminate mainly the $\chi_i^0\text{-}\chi_j^0$ background. Our analysis shows that this cut is rather effective in this respect; the event rate is reduced by almost 50%. Surprisingly, it also reduces the $\tilde{\nu}_{\tau_L}\text{-}\chi_{1/2}^0$ background by a considerable amount. The reason for this is the following: $\tilde{\nu}_{\tau_L}\text{-}\chi_{1/2}^0$ is produced in cascade decays of squarks and gluinos and the $\tilde{\nu}_{\tau_L}$ is often produced from a χ_1^\pm (the branching fraction being 30% or more in some BPs). In that case the decay process is $\chi_1^\pm \rightarrow \tau^\pm \tilde{\nu}_{\tau_L}$. The τ out of such a χ_1^\pm is sometimes identified, whereas the τ out of a $\chi_{1/2}^0$ ($\chi_{1/2}^0 \rightarrow \tau^\pm \tilde{\tau}^\mp$) from the other decay chain goes untagged. The invariant mass distribution of a track and the jet coming from an unidentified τ is clustered around $m_{\chi_i^0}$ ($i = 1, 2$). Thus cut X turns out to be effective in eliminating this type of background.

After all this effort, however, one is still left with background events which smear the sharp fall in the transverse mass distribution of the $\tilde{\tau}\nu_\tau$ pair. We have to impose an additional cut on the transverse mass distribution to separate it from the background. This is in the form of the demand $M_{\tilde{\tau}\nu_\tau}^T > \frac{3}{4}m_{\chi_2^0}$, whereby it is possible to reduce these backgrounds further, as can be seen from Tables II and III. It is then possible to determine the chargino mass ($m_{\chi_1^\pm}$) by looking at the peak, followed by a sharp descent, in the transverse mass distribution for several benchmark points.

The transverse mass distributions for different benchmark points are shown in Figs. 5 and 6. The τ -identification efficiency is assumed to be 50% in Fig. 5; Fig. 6 reflects the improvement achieved in a relatively optimistic situation when this efficiency is 70%.

At BP1 the statistics is very poor and we have relatively few events within a bin of 40 GeV around $m_{\chi_1^\pm}$. One has about 50% of the events coming from other SUSY processes (Table II). Additionally, the sharp edge is not clearly visible due to the presence of a large number of $\chi_1^0\chi_1^0$ events, even after imposing the $M_{\tilde{\tau}\nu_\tau}^T > \frac{3}{4}m_{\chi_2^0}$ cut.

The situation is similar for BP2 as well. In BP3 and BP4 a peaklike behavior, followed by a sharp fall, is considerably more distinct, from which one can extract the value of $m_{\chi_1^\pm}$.

For BP5 and BP6 the contamination due to the SUSY background is found to be small compared to the other benchmark points. The χ_1^\pm production rate in cascade decays of squarks/gluinos is also higher there. Hence the transverse mass distribution shows a distinctly sharp fall, from which a faithful reconstruction of chargino mass is possible.

As a comparison between Figs. 5 and 6 shows, the prospect can be improved noticeably if one has a better

τ -identification efficiency ($\epsilon_\tau = 70\%$). In such a case, the background from $\chi_1^0\text{-}\chi_1^0/\chi_1^0\text{-}\chi_2^0/\chi_2^0\text{-}\chi_2^0$ is less severe compared to the case where the τ -identification efficiency is 50%.

From Figs. 5 and 6, one can also see some small peaks in the $M_{\tilde{\tau}\nu_\tau}^T$ distribution with very few event rate, in the region where $M_{\tilde{\tau}\nu_\tau}^T > m_{\chi_2^0}$. This can be attributed to those events where a χ_3^0 or a χ_4^0 decays into a $\tilde{\tau}\tau$ pair, and also to the production of the heavier chargino.

V. SUMMARY AND CONCLUSIONS

We have considered a SUSY scenario where the LSP is dominated by a right-sneutrino state, while a dominantly right-chiral stau is the NLSP. The stau, being stable on the length scale of collider detectors, gives rise to charged tracks, the essence of SUSY signal in such a scenario. It is also shown that such a spectrum follows naturally from a high-scale scenario of universal scalar and gaugino masses.

We have extended our earlier study on the mass reconstruction of nonstrongly interacting superparticles in such cases, by considering final states resulting from the decays of a $\chi_1^\pm\chi_{1(2)}^0$ pair in SUSY cascades. The final state under consideration is $\tau_j + 2\tilde{\tau}$ (opposite-sign charged tracks) + $\cancel{E}_T + X$. We have systematically developed a procedure for identifying the contribution to \cancel{p}_T from the neutrino produced in χ_1^\pm decay, together with a quasistable stau. Once this is possible, the transverse mass distribution of the corresponding $\tilde{\tau} - \nu_\tau$ pair can be extracted from data at the LHC, and a sharp edge in that distribution yields information on the chargino mass. While eliminating the SM backgrounds in this process is straightforward, we have suggested ways of minimizing the contamination of the relevant final state from competing processes in the same SUSY scenario. Selecting a number of benchmark points in the parameter space, we show in which regions the above procedure works. In cases where it does not, the main causes of failure are identified as the overwhelmingly large contribution from χ_1^0 pairs, and, for example, in the first two benchmark points, somewhat poor statistics. The other important issue is the differentiation between the χ_1^0 and the χ_2^0 produced in association with the χ_1^\pm . For this, we make use of the assumption of gaugino universality as well as the information extracted from the effective mass distribution in SUSY processes.

To conclude, the existence of quasistable charged particles, a possibility not too far-fetched, opens a new vista in the reconstruction of superparticle masses. We have repeatedly suggested utilization of this facility in our works on gluino [6] and neutralino [13] mass reconstruction. This work underscores a relatively arduous task in this respect, in obtaining transverse mass edges in chargino decays. In spite of rather challenging obstacles from underlying SUSY processes, we demonstrate the feasibility of our

procedure, which is likely to be enhanced by improvement in, for example, the W - and τ -identification efficiencies.

ACKNOWLEDGMENTS

This work was partially supported by funding available from the Department of Atomic Energy, Government of

India for the Regional Centre for Accelerator-based Particle Physics, Harish-Chandra Research Institute. Computational work for this study was partially carried out at the cluster computing facility of Harish-Chandra Research Institute.

-
- [1] For reviews see, for example, H. E. Haber and G. L. Kane, Phys. Rep. **117**, 75 (1985).
- [2] S. Dawson, E. Eichten, and C. Quigg, Phys. Rev. D **31**, 1581 (1985); X. Tata, arXiv:hep-ph/9706307; M. E. Peskin, arXiv:0801.1928.
- [3] K. Hamaguchi, M. M. Nojiri, and A. de Roeck, J. High Energy Phys. 03 (2007) 046.
- [4] T. Schwetz, M. Tortola, and J. W. F. Valle, New J. Phys. **10**, 113011 (2008); G. L. Fogli *et al.*, Phys. Rev. D **78**, 033010 (2008); A. Bandyopadhyay, S. Choubey, S. Goswami, S. T. Petcov, and D. P. Roy, arXiv:0804.4857.
- [5] C. L. Chou and M. E. Peskin, Phys. Rev. D **61**, 055004 (2000).
- [6] D. Choudhury, S. K. Gupta, and B. Mukhopadhyaya, Phys. Rev. D **78**, 015023 (2008).
- [7] S. K. Gupta, B. Mukhopadhyaya, and S. K. Rai, Phys. Rev. D **75**, 075007 (2007).
- [8] A. H. Chamseddine, R. L. Arnowitt, and P. Nath, Phys. Rev. Lett. **49**, 970 (1982).
- [9] M. Kawasaki, K. Kohri, and T. Moroi, Phys. Lett. B **649**, 436 (2007).
- [10] C. Amsler *et al.* (Particle Data Group), Phys. Lett. B **667**, 1 (2008).
- [11] E. Komatsu *et al.*, Astrophys. J. Suppl. Ser. **180**, 330 (2009).
- [12] T. Asaka, K. Ishiwata, and T. Moroi, Phys. Rev. D **73**, 051301 (2006); T. Asaka, K. Ishiwata, and T. Moroi, Phys. Rev. D **75**, 065001 (2007).
- [13] S. Biswas and B. Mukhopadhyaya, Phys. Rev. D **79**, 115009 (2009).
- [14] J. Smith, W. L. van Neerven, and J. A. M. Vermaseren, Phys. Rev. Lett. **50**, 1738 (1983).
- [15] J. L. Feng, A. Rajaraman, and F. Takayama, Phys. Rev. Lett. **91**, 011302 (2003); J. L. Feng, A. Rajaraman, and F. Takayama, Phys. Rev. D **68**, 063504 (2003); J. R. Ellis, K. A. Olive, Y. Santoso, and V. C. Spanos, Phys. Lett. B **588**, 7 (2004); J. L. Feng, S. Su, and F. Takayama, Phys. Rev. D **70**, 075019 (2004); A. Ibarra and S. Roy, J. High Energy Phys. 05 (2007) 059.
- [16] S. Dimopoulos, M. Dine, S. Raby, and S. D. Thomas, Phys. Rev. Lett. **76**, 3494 (1996); D. A. Dicus, B. Dutta, and S. Nandi, Phys. Rev. Lett. **78**, 3055 (1997); S. Ambrosiano, G. D. Kribs, and S. P. Martin, Phys. Rev. D **56**, 1761 (1997); D. A. Dicus, B. Dutta, and S. Nandi, Phys. Rev. D **56**, 5748 (1997); K. M. Cheung, D. A. Dicus, B. Dutta, and S. Nandi, Phys. Rev. D **58**, 015008 (1998); J. L. Feng and T. Moroi, Phys. Rev. D **58**, 035001 (1998); P. G. Mercadante, J. K. Mizukoshi, and H. Yamamoto, Phys. Rev. D **64**, 015005 (2001).
- [17] A. V. Gladyshev, D. I. Kazakov, and M. G. Paucar, Mod. Phys. Lett. A **20**, 3085 (2005); T. Jittoh, J. Sato, T. Shimomura, and M. Yamanaka, Phys. Rev. D **73**, 055009 (2006).
- [18] S. P. Martin, arXiv:hep-ph/9709356, and references therein.
- [19] S. P. Martin and P. Ramond, Phys. Rev. D **48**, 5365 (1993).
- [20] N. Arkani-Hamed, L. J. Hall, H. Murayama, D. Tucker-Smith, and N. Weiner, Phys. Rev. D **64**, 115011 (2001).
- [21] D. L. Rainwater, D. Zeppenfeld, and K. Hagiwara, Phys. Rev. D **59**, 014037 (1998).
- [22] G. Aad *et al.* (ATLAS Collaboration), arXiv:0901.0512.
- [23] F. E. Paige, S. D. Protopopescu, H. Baer, and X. Tata, arXiv:hep-ph/0312045.
- [24] A. Djouadi, M. Drees, and J. L. Kneur, J. High Energy Phys. 03 (2006) 033.
- [25] T. Sjostrand, S. Mrenna, and P. Skands, J. High Energy Phys. 05 (2006) 026.
- [26] H. L. Lai *et al.* (CTEQ Collaboration), Eur. Phys. J. C **12**, 375 (2000).
- [27] W. Beenakker, R. Hopker, M. Spira, and P. M. Zerwas, Nucl. Phys. **B492**, 51 (1997).
- [28] C. G. Lester and D. J. Summers, Phys. Lett. B **463**, 99 (1999).
- [29] B. Gripaios, J. High Energy Phys. 02 (2008) 053; H. C. Cheng and Z. Han, J. High Energy Phys. 12 (2008) 063; A. J. Barr, B. Gripaios, and C. G. Lester, arXiv:0908.3779.
- [30] Y. Coadou *et al.*, ATLAS Internal Note No. ATL-PHYS-98-126.
- [31] CMS Collaboration, CMS-TDR-8.1; CERN/LHCC 2006-001
- [32] S. Asai *et al.*, Eur. Phys. J. C **32S2**, s19 (2004).
- [33] W. Beenakker, S. Dittmaier, M. Kramer, B. Plumper, M. Spira, and P. M. Zerwas, Nucl. Phys. **B653**, 151 (2003).